THE JOURNAL OF PHYSICAL CHEMISTRY A

pubs.acs.org/JPCA Article

Metalated Porphyrin Stable Free Radicals: Exploration of Electron Spin Communication and Dynamics

Norbert Grzegorzek, Haochuan Mao, Patrick Michel, Marc J. Junge, Emmaline R. Lorenzo, Ryan M. Young, Matthew D. Krzyaniak, Michael R. Wasielewski, and Erin T. Chernick*

Cite This: J. Phys. Chem. A 2020, 124, 6168–6176 Read Online

ACCESS | Metrics & More | Article Recommendations | Supporting Information

ABSTRACT: Switchable coupling between two qubits is important for quantum information science (QIS). As a proof of concept, a series of mesosubstituted porphyrins have been synthesized with a (2,2,6,6-tetramethylpiperidin-1-yl)oxyl stable free radical (SFR) appended and metalated with Cu(II), Ni(II), and Zn(II) in order to explore the interaction between the SFR doublet state and metalloporphyrin. The spin state of the porphyrin varies upon metal insertion, where Zn(II) is a diamagnetic metal, Cu(II) is paramagnetic, and Ni(II) can be switched from a diamagnetic square-planar structure to a paramagnetic octahedral state by complexation with a solvent (i.e., pyridine or tetrahydrofuran). Time-resolved electron paramagnetic resonance (EPR) measurements reveal that upon photoexcitation, the Zn(II) and free-base porphyrin species demonstrate different magnetic exchange regimes between the porphyrin triplet excited states and the SFR doublet state, with the Zn derivative populating a quartet state (i.e., moderate magnetic exchange), whereas the free-base derivative remains a triplet (i.e., weak magnetic exchange). Transient absorption measurements corroborate the TREPR results, demonstrating a 66% increase in the singlet excited-state decay rate due to enhanced intersystem crossing for the Zn(II) derivative in comparison to a modest 14% enhancement for the free-base porphyrin. These results enable the realization of a switchable qubit coupler, depending upon Zn metal insertion to the free-base porphyrin, which has potential QIS applications.

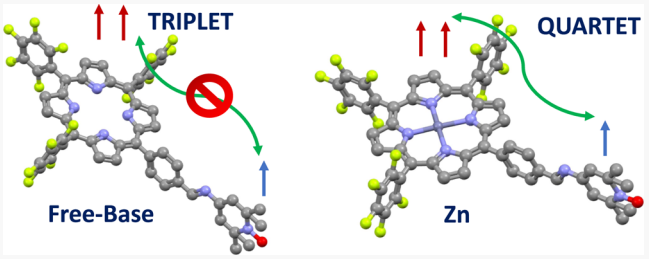

INTRODUCTION

World energy consumption is ever increasing, and new methods and developments are required to harvest renewable energy to keep costs down as well as preserve Earth's natural resources. Effective organic electronic devices operating on a renewable energy platform will face challenges with time, as the device operating sizes drop below the 10 nm size range.[1] At this reduced size scale, operational principles transition to the single molecule regime and become quantized in nature. Consequently, the research field of spintronics and quantum information science (QIS) has been gaining ever-increasing momentum, where information can be manipulated, stored, and transferred using the quantum properties of electron spins.[2,3]

The term spintronics was first introduced in the 1980s and has evolved into the field of QIS where electron spins have been demonstrated to serve as quantum bits (qubits) in a variety of applications.[3] However, research pertaining to this field is still in its infancy with respect to predictable and reliable molecular design for organic QIS applications. Advanced fundamental studies are required to elucidate the molecular properties necessary to achieve practical operational devices functioning to manipulate quantum information. From an organic synthesis perspective, attention has been focused on the creation of a diverse range of organic molecules with interesting open-shell character, which have targeted QIS applications.[4−12]

Porphyrins represent a class of aromatic, light-harvesting chromophores that can coordinate metals, transforming them to organometallic species with further unique chemical and physical properties.[13] Porphyrins can also exist as stabile oxidized, reduced, or neutral radicals.[14] From a biological perspective, extensive research on oxophlorin and *meso*-hydroxyporphyrin has been carried out to elucidate their role in the catabolism of heme.[15] Inspired by Nature, impressive synthetic achievements have been made in the design and realization of stable porphyrin oxyl radicals with relevant magnetic properties.[16,17]

Porphyrins can be metalated with numerous metals, including Zn(II), Ni(II), and Cu(II). These metals can provide a platform for studying the electron spin dynamics

Received: April 9, 2020
Revised: June 12, 2020
Published: June 17, 2020

https://dx.doi.org/10.1021/acs.jpca.0c03176
J. Phys. Chem. A 2020, 124, 6168–6176

of both diamagnetic and paramagnetic porphyrin complexes: Zn(II) is a diamagnetic metal, Ni(II) can switch between diamagnetic and paramagnetic states depending on ligation,[18,19] and Cu(II) is paramagnetic.

The intermolecular[20−23] and intramolecular interactions[24,25] between a stable doublet radical and a porphyrin triplet state have both been investigated by time-resolved electron paramagnetic resonance (TREPR). Different effects of a stable free radical (SFR) on a photoexcited chromophore or charge-transfer state have been observed[26] such as enhanced intersystem crossing (EISC)[27] and electron spin polarization transfer.[28] These mechanisms are governed by the molecular and electronic structure as well as the extent of magnetic exchange coupling between the porphyrin triplet state and the SFR.

Van der Est et al. reported a transient EPR study on a *meso*-tetratolylporphyrin complex with a verdazyl SFR appended directly to the *β*-position of the porphyrin.[24] The porphyrin derivative was then metalated with vanadium to incorporate an additional unpaired spin to the system. TREPR spectroscopy revealed that the free-base porphyrin triplet state couples ferromagnetically with the doublet radical to form a quartet species. For vanadium porphyrin, the verdazyl radical couples ferromagnetically to the porphyrin triplet but antiferromagnetically to the unpaired spin of the vanadium metal. These results are very relevant when addressing current research efforts toward the design of molecular systems that can undergo spin hyperpolarization where the polarization of the excited state is transferred to the SFR.[29−34]

Not only the porphyrin metal center but also the substituents and their position around the porphyrin periphery largely influence the spin−spin exchange between a doublet state and a porphyrin.[35] For example, Balch et al. reported that a *β*-octaethylporphyrin Ni(II) oxyl radical complex demonstrated an antiferromagnetic interaction between the oxyl radical and paramagnetic Ni(II) center.[36] However, when Osuka et al. substituted a porphyrin oxyl radical with pentafluorophenyl substituents in the mesopositions, the oxyl radical demonstrated a ferromagnetic interaction with the high-spin Ni(II).[37]

We are specifically interested in exploring the spin−spin interactions between an SFR covalently appended to a photoexcited chromophore.[38−42] Specifically, we want to design and synthesize molecular systems where the spin states can be manipulated such that the magnetic exchange coupling between the radical and photoexcited chromophore can be turned "on" and "off". The final goal is to design and synthesize functional organic molecules with controllable variable magnetic exchange regimes that may be relevant for quantum information applications.

Based on the aforementioned reports, we decided to elaborate upon the porphyrin and synthesize a series of metalloporphyrins with an SFR covalently appended to the mesoposition, where the spin state of the metal can be varied. Herein reported is the synthesis of a series of mesosubstituted porphyrins with the electron-withdrawing pentafluorobenzene moiety in three positions to aid in pyridine coordination to form the Ni(II) octahedral high-spin state. Electron-withdrawing groups on the periphery of the macrocycle decrease the porphyrin basicity and enhance the interaction between the Ni ion and axial nitrogen donor ligands.[37,43−45] The final mesoposition substituted with a (2,2,6,6-tetramethylpiperidin-1-yl)oxyl (TEMPO) SFR appended by an imine bond between a phenyl group and the porphyrin core (Figure 1). The phenyl group ensures that the radical substituent assumes a nearly

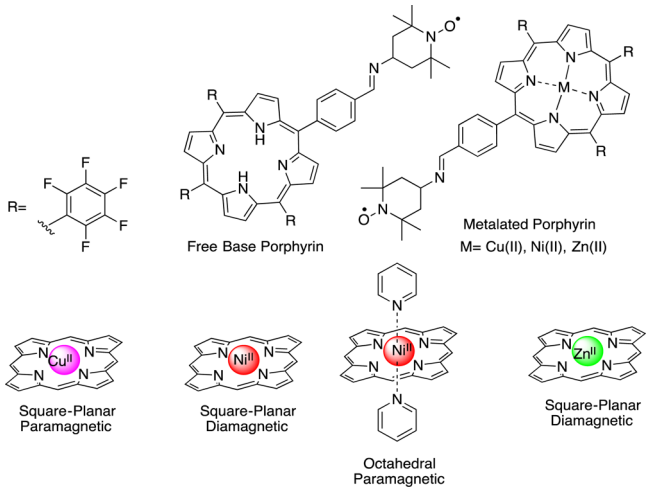

Figure 1. Target porphyrin radicals and their metal-coordination motifs.

perpendicular conformation relative to the porphyrin chromophore. The porphyrin was metalated with Cu(II), Zn(II), and Ni(II), whose spin states have been described earlier. The complete synthesis and characterization of the free base and three metalloporphyrins are reported, in addition to TREPR and transient absorption (TA) measurements. We have been able to show that the free base and zinc porphyrin radicals demonstrate different magnetic exchange regimes in the excited state. Based on transient nutation experiments, we were able to demonstrate[29] that the Zn derivative populates a quartet state, indicating that the porphyrin triplet state and doublet radical are coupled, whereas the free-base excited state is a triplet, demonstrating weak magnetic exchange. Additional TA measurements corroborate the TREPR results, demonstrating a much larger increase in percentage of intersystem crossing (ISC) rates of the metalated porphyrin in comparison to the free-base porphyrin. These results permit us to envision a switchable quantum state based upon metalation of the porphyrin with Zn(II).

RESULTS AND DISCUSSION

Synthesis. The synthesis of mesosubstituted porphyrins is well documented, with methodology milestones reported by Rothemund,[46] Adler,[47] and Lindsey.[48] Substitution of a porphyrin with different functional groups is highly dependent on the number and reactivity of functionalities desired to comprise the porphyrin and the final configuration of the functionalities (i.e., asymmetric or cis/trans).[49−55] Our desired porphyrin requires three pentafluorophenyl substituents and one cyanophenyl substituent,[56] which serves as a synthetic handle for further reactions. Shown in Scheme 1 is the porphyrin condensation reaction with the pentafluorophenyl dipyrromethane, *p*-cyanobenzaldehyde, and pentafluorobenzaldehyde starting reagents in the presence of the Lewis acid trifluoroborate. Oxidation with 2,3-dichloro-5,6-dicyano-1,4-benzoquinone (DDQ) yields desired precursor porphyrin **1** in 18% yield following purification.

Porphyrin **1** is treated with diisobutylaluminum hydride (DIBAL-H) to afford the free-base porphyrin aldehyde **2** in

https://dx.doi.org/10.1021/acs.jpca.0c03176
J. Phys. Chem. A 2020, 124, 6168−6176

Scheme 1. Synthetic Route toward Precursor Porphyrin 1; (a) (i) $BF_3 \times Et_2O$, 1 h, rt and (ii) DDQ (3 equiv), 1 h, rt (18%)

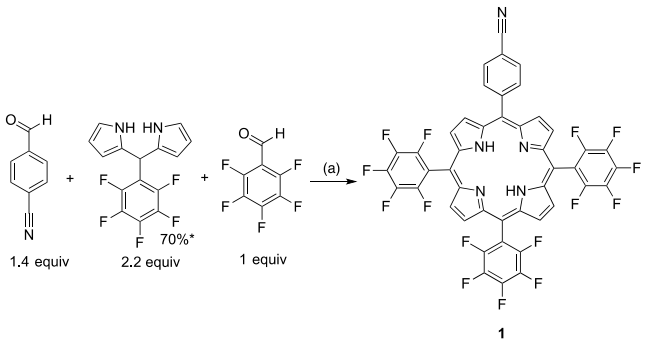

37% yield (Scheme 2). The principal side reaction is insertion of the aluminum metal from the DIBAL-H reduction reagent into the porphyrin core, which is very difficult to remove after insertion.[57] Hence, a synthetic methodology was developed to protect the porphyrin core with Zn (Scheme 2) and simultaneously allowed for the isolation of the Zn radical. Concurrently, we recovered the unprotected porphyrin aldehyde precursor **2** in higher yields compared to direct reduction from the cyanophenyl free-base porphyrin precursor **1**.

Free-base porphyrin **1** was refluxed with zinc(II) acetate dihydrate to afford **1(Zn)** in the near-quantitative yield (99%), which was then reduced with DIBAL-H to the corresponding aldehyde **2(Zn)** in 93% yield. From porphyrin **2(Zn)**, free-base aldehyde **2** was recovered in 95% yield by treatment with trifluoroacetic acid (TFA). Aldehyde **2** was then further reacted to free-base radical **3**. Appending the TEMPO SFR is accomplished following a previously reported procedure.[38] Ultrasonication of porphyrin aldehyde precursors **2** and **2(Zn)** with excess TEMPO-amine in DCM with an acid catalyst yields free-base porphyrin radical **3** and Zn porphyrin radical **3(Zn)** in the near-quantitative yield.[58] Removal of excess TEMPO-amine is accomplished via size exclusion chromatography as the imine bond undergoes hydrolysis back to the starting material under acidic (silica gel) or basic (alumina gel) purification conditions.

The final two metalated porphyrins (Cu and Ni) were synthesized from either cyanophenyl free-base porphyrin **1** or free-base benzaldehyde porphyrin **2**, as shown in Scheme 3. Porphyrin **1** or **2** can undergo metal insertion by copper(II) acetate to form the corresponding copper metalated derivatives **1M** (M = Cu-94%) and **2M** (M = Cu-88%) via methods (b) and (c). Conversely, free-base porphyrin **1** was metalated with Cu and then reduced with DIBAL-H as outlined in procedure (d) to yield **2(Cu)** in 74%. Porphyrin **2(Ni)** was achieved by metalation of free-base aldehyde **2** with nickel(II) acetate. Porphyrin radical precursors **2(Cu)** and **2(Ni)** are subjected to the TEMPO amine condensation reaction described earlier to yield porphyrin radicals **3(Cu)** and **3(Ni)** in the near-quantitative yield.

Steady-State Spectroscopy. Steady-state UV/vis absorption measurements were carried out on **3**, **3(Ni)**, **3(Zn)**, and **3(Cu)** in DCM (see the Supporting Information pgs S22–S24). The Soret band absorption has maxima at 415, 407, 416, and 411 nm for **3**, **3(Ni)**, **3(Zn)**, and **3(Cu)**, respectively. Free-base porphyrin radical **3** displays Q-band absorptions at 509, 541, and 585 nm. The three metalated porphyrin radicals have two Q-band absorptions, as expected,[59] at 525/558, 545/

Scheme 2. Synthesis toward Radicals 3 and 3(Zn); (a) (i) DIBAL-H (2 equiv), DCM, 110 min, rt, Ar and (ii) $NH_4Cl_{aq.}$ sat., 40 min, rt (37%); (b) $Zn(OAc)_2 \times 2H_2O$ (10 equiv), $CHCl_3$/MeOH, 2 h, 85 °C (99%); (c) (i) DIBAL-H (4 equiv), DCM, 120 min, rt, Ar and (ii) $NH_4Cl_{aq.}$ sat., 40 min, rt (95%); (d) (i) TFA, DCM, rt and (ii) H_2O, rt, 15 min (93%); and (e) TEMPO–Amine (10 equiv), AlO_x (Excess), DCM, 2 h Sonication (≥95%)

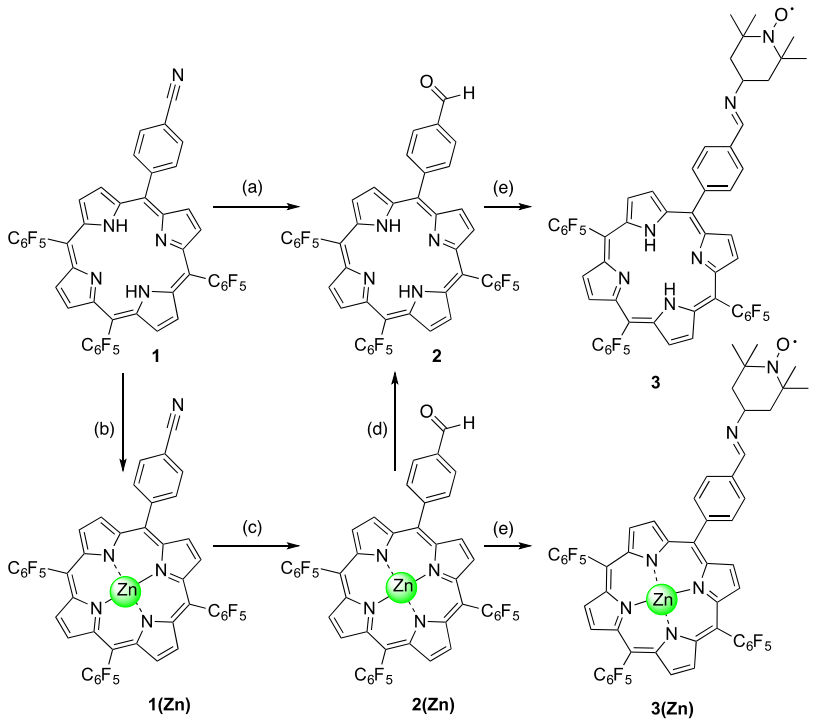

https://dx.doi.org/10.1021/acs.jpca.0c03176
J. Phys. Chem. A 2020, 124, 6168–6176

Scheme 3. Synthesis toward Radicals 3(Cu) and 3(Ni); (a) (i) DIBAL-H (2 equiv), DCM, 110 min, rt, Ar and (ii) $NH_4Cl_{aq.}$ sat., 40 min, rt (37%); (b) (Cu) − $Cu(AcO)_2 \times H_2O$ (5 equiv), $CHCl_3$/MeOH, 1 h, 85 °C (94%); (c) (i) (Cu) $Cu(AcO)_2 \times H_2O$ (5 equiv), $CHCl_3$/MeOH, 1 h, 85 °C (88%) and (ii) (Ni) $Ni(AcO)_2 \times 4H_2O$ (15 equiv), Glacial Acetic Acid, 6 h, 130 °C (84%); (d) (i) DIBAL-H (4 equiv), DCM, 120 min, rt, Ar (Cu 74%); and (e) TEMPO−Amine (10 equiv), AlO_x (Excess), DCM, 2 h Sonication (≥95%)

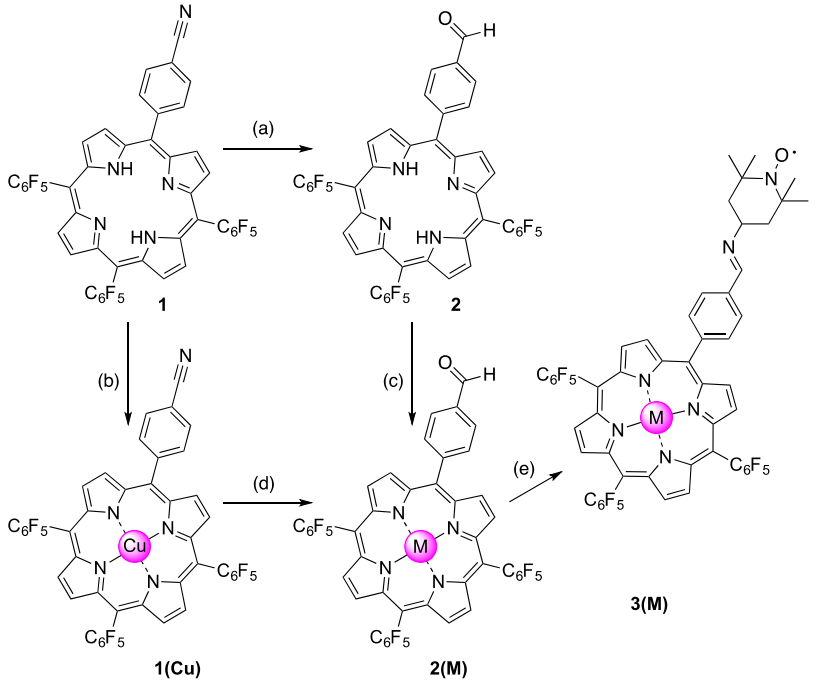

577, and 536/571 nm for **3(Ni)**, **3(Zn)**, and **3(Cu)**, respectively. Comparison of the UV/vis spectra of the four radicals to their aldehyde precursors shows no discernible difference in absorption maxima, indicating that the radical has negligible electronic influence.

Steady-state continuous wave EPR (CW-EPR) measurements were conducted for **3**, **3(Zn)**, **3(Ni)**, and **3(Cu)** at the X band (9.5 GHz). The spectra collected at 85 K are shown in Figure 2, and those collected at room temperature are provided in the Supporting Information (Figures S23−S25). Free-base porphyrin **3** and **3(Zn)** are diamagnetic; hence, only the powder spectra of the TEMPO free radical are detected. For **3(Ni)**, it is assumed that two *m*THF molecules coordinate to

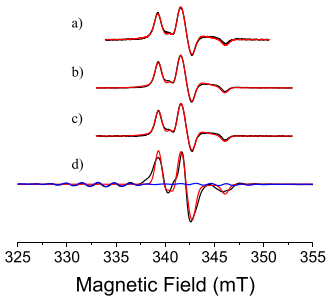

Figure 2. Steady-state CW-EPR of (a) **3**, (b) **3(Zn)**, (c) **3(Ni)**, and (d) **3(Cu)** in *m*THF at the X band (9.5 GHz), obtained at 85 K with a 0.1 mT modulation amplitude. Overlaid in red are the simulations for the TEMPO; all four simulations utilized the same fit parameters: g = [2.0112, 2.0083, 2.0034] and A(14N) = [17.9, 17.9, 93.8] MHz. Shown in blue is the simulation for the copper porphyrin utilizing the parameters g = [2.069, 2.069, 2.186], A(Cu) = [79, 79, 611] MHz, and 4 equiv A(N) = [48, 48, 43] MHz.

Ni, making it octahedral and paramagnetic in nature. However, the zero-field splitting (zfs) between the two unpaired electrons of Ni renders the metal EPR silent at the X band (9.5 GHz),[19,60] and again, we only observe the TEMPO radical. The spectrum of **3(Cu)** show an additional multiplet at a lower field because of hyperfine coupling of the copper unpaired electron with the four porphyrin ^{14}N nuclei, which is characteristic of copper porphyrins.[61,62]

Time-Resolved Spectroscopy. TREPR measurements were performed at 85 K in glassy *m*THF following photoexcitation at the most intense Q-band absorption ($S_1 \leftarrow S_0$ transition) for each sample.[63] Porphyrins **3(Ni)** and **3(Cu)** did not yield any TREPR signals, which is most likely due to the strong spin−orbit (SO) coupling between the paramagnetic metal center and the porphyrin core,[64] leading to enhanced ISC,[27,30,65] which shortens the lifetime of the porphyrin triplet excited states (vide infra). Shown in Figure 3a,b are the TREPR spectra of **2**, **3**, **2(Zn)**, and **3(Zn)** recorded at 40 ns following excitation. Free-base porphyrin **2** gives an EPR spectrum with an e,a,e,a,e,a (a = enhanced absorption, e = enhanced emission) polarization pattern (Figure 3a upper), which is the result of selectively populating the $|T_y\rangle$ triplet sublevel due to SO-ISC.[66] Overlaid in red is a simulation of the triplet using the zfs parameters: $|D|$ = 1294 MHz and E/D = 0.118, which falls within the range expected for a free-base porphyrin.[67,68] The spectrum of **3** exhibits the same polarization and has largely the same spectral shape as **2** with the exception of a small negative peak at 338 mT. This negative peak can be attributed to some nonzero coupling between the TEMPO radical and the triplet;[69,70] however, the small amplitude and lack of other spectral changes make simulating the spectrum underdetermined. Porphyrin **2(Zn)** (Figure 3b) shows an a,a,a,e,e,e polarization pattern, which is consistent

https://dx.doi.org/10.1021/acs.jpca.0c03176
J. Phys. Chem. A 2020, 124, 6168−6176

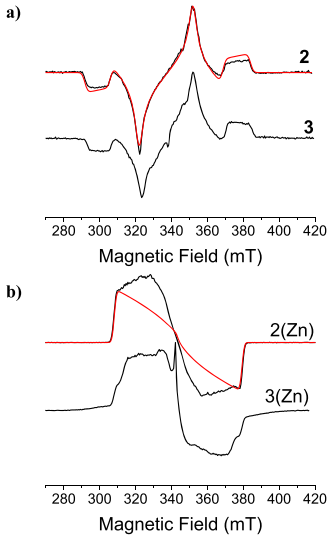

Figure 3. TREPR spectra in frozen *m*THF at 85 K at 40 ns following a 7 ns laser pulse for (a) **2** and **3** and (b) **2(Zn)** and **3(Zn)**.

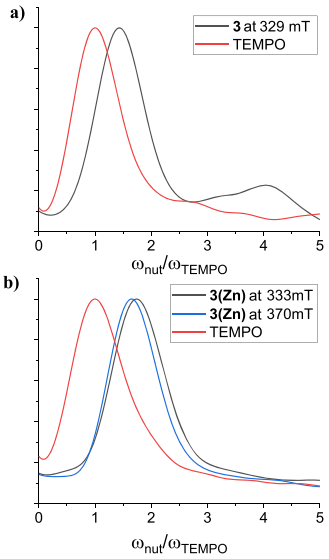

Figure 4. Echo-detected transient nutation spectra collected at 85 K in *m*THF for (a) **3** and (b) **3(Zn)** following the 510 and 550 nm, 7 ns, and 2.5 mJ laser pulse, respectively.

with selective population of the $|T_z\rangle$ triplet sublevel. Simulation of the triplet spectrum yields the zfs parameters: $|D| = 995$ MHz and $E/D = 0.332$ and agrees well with reports on similar molecules.[71,72] The deviation of the simulation from the spectrum is likely due to some aggregation;[72] however, we do not anticipate aggregation to have a major effect on the zfs parameters unless there is significant delocalization.[73−75] The spectrum of **3(Zn)** shows significant changes relative to **2(Zn)** including a 5 mT splitting on the outer features, with a wider set of wings along with a strong narrow absorptive line at 342 mT. In order to confirm that these features are not a result of aggregation, a TREPR spectrum of **3(Zn)** in the presence of a coordinating ligand, pyridine, was also collected (Figure S28); interestingly, no significant change in the structure was observed. Additionally, the central peaks in both **3** and **3(Zn)** decay concomitantly with the broad features (Figure S27), which suggests that the central peak is a result of a spin-coupled quartet species and not from transfer of polarization from the triplet to TEMPO.

In order to further investigate the spin states of **3** and **3(Zn)**, pulsed transient nutation EPR spectroscopy was performed. This technique provides information about the electron spin quantum number and the transition by measuring the nutation frequency of a spin upon irradiation with resonant microwaves.[76,77] Molecules **3** and **3(Zn)** are ideally suited for transient nutation spectroscopy because in the dark state, they have an internal $S = 1/2$ standard by way of TEMPO, which then allows for normalization of the nutation frequency and easy comparison to the photogenerated state. Figure 4a,b shows the nutation spectra acquired at the noted magnetic field points for **3** and **3(Zn)**, respectively. The nutation frequency of the TEMPO radical, shown in red, was collected prior to photoexcitation; following photoexcitation, the nutation frequencies of the transient EPR features were collected and normalized to the frequency of the $S = 1/2$ TEMPO radical. Hence, $\omega = 1$ corresponds to the $m_s = -1/2$ to $m_s = 1/2$ transition for an $S = 1/2$ species. In Figure 4a, the feature at 329 mT for **3** has a nutation frequency of $\omega = 1.4 \approx \sqrt{2}$, which corresponds to the $m_s = \pm 1$ to $m_s = 0$ transitions of an $S = 1$ triplet state. At 333 mT and 370 mT in **3(Zn)** (Figure 4b), the nutation frequencies are $\omega = 1.7$ and $\omega = 1.65$, respectively, which correspond closely to the expected frequency of the $m_s = \pm 1/2$ to $m_s = \pm 3/2$ transitions for an $S = 3/2$ quartet species, $\sqrt{3}$.

The combination of the TREPR and the transient nutation results provides an estimation of the magnitude of the exchange coupling between the triplet and radical (J_{TR}) in the excited states of **3** and **3(Zn)**. The central feature in the TREPR spectrum of **3** provides evidence for coupling between the triplet and the radical; however, the transient nutation suggests that the photogenerated triplet is only weakly interacting with TEMPO and the character of the EPR spectrum remains essentially that of separate triplet and radical species. In this case, the combination of triplet−radical dipolar coupling and J_{TR} is much smaller than the triplet zfs and likely smaller than the inhomogeneous line width of the TREPR spectrum.[69,70,78]

In contrast, the TREPR spectrum of **3(Zn)** more obviously demonstrates a coupling between the triplet and radical, and the nutation frequencies clearly show that the quartet is an eigenstate of the spin Hamiltonian.[69,70] The spectral width of the TREPR spectrum of **3(Zn)** does not contract by 2/3 as would be expected of a strongly coupled triplet−radical quartet, which places the coupling into the weak-to-moderate regime. In comparison to **3**, the triplet−radical dipolar coupling should not change significantly in **3(Zn)**, meaning that J_{TR} in **3(Zn)** must have increased. This increase in J_{TR} from **3** to **3(Zn)** can be explained by an increase in delocalization of the triplet wave function with the addition of Zn.[79] This is immediately apparent with a comparison of the zfs values for **2** and **2(Zn)**, which are 1294 and 995 MHz, respectively. Using the point dipole approximation,[80] the mean distance between the two triplet electrons increases from 3.42 to 3.72 Å when the porphyrin is metalated with Zn; this change suggests that the π-system containing the triplet is larger in **2(Zn)**.[81,82] Free-base porphyrins are also known to have a nonplanar structure as opposed to the more planar zinc porphyrin,[83,84] which also results in less orbital overlap and thus a decrease of the exchange interaction with the appended radical.

https://dx.doi.org/10.1021/acs.jpca.0c03176
J. Phys. Chem. A 2020, 124, 6168−6176

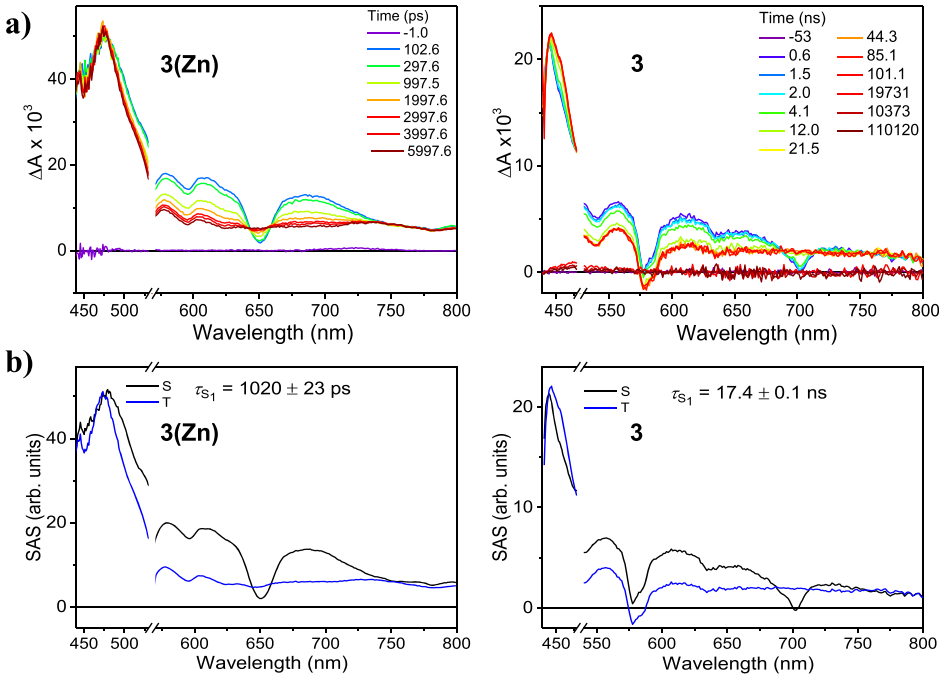

Figure 5. TA spectra and species-associated spectra of **3** and **3(Zn)**. (a) TA spectra of **3** and **3(Zn)** in 2-methyl THF at 85 K following λ_{ex} = 550 nm and λ_{ex} = 510 nm, respectively. (b) Species-associated spectra of **3** and **3(Zn)** resulting from the global fitting of the data to an A → B model.

The increase in J_{TR} manifests itself through changes of the TREPR spectrum of **3(Zn)** relative to **2(Zn)** and broad wings extending out 20 mT from a more intense central feature with approximately the same width as **2(Zn)**. Simulations suggest that when J_{TR} is large but still less than the triplet zfs, broad wings arise and can provide an indication of the maximum magnitude of J_{TR}, as illustrated in Figure S29. Based on the simulations, J_{TR} is at most 20 mT (560 MHz); however, the weak and unstructured nature of the wings suggests a distribution of J_{TR} which is not surprising, given the flexible nature of both TEMPO and the linker. The magnitude of J_{TR} and the distribution are not without a precedent; a similarly linked biradical demonstrated an exchange interaction that ranged from 10 mT (280 MHz) to more than 40 mT (1000 MHz) as a function of temperature, and this range was attributed to the flexible nature of both the linker and TEMPO.[85,86]

TA spectroscopy studies on **2**, **3**, **2(Zn)**, and **3(Zn)** determined the effect of EISC on the singlet excited-state lifetimes of the free-base porphyrin and zinc porphyrin in the presence of nitroxide radicals. Comparison of the relative quenching rates provides qualitative information on the exchange coupling between the nitroxide radical and porphyrin triplet state. The TA apparatus is detailed in the Supporting Information. Photoexcitation of **3** and **3(Zn)** in *m*THF at 85 K populates the excited singlet state of the Zn porphyrin or free-base porphyrin, followed by ISC to the porphyrin triplet states as seen by the depletion of the stimulated emission at 650 nm for **3** and 700 nm for **3(Zn)** (Figure 5.). Global fitting of the spectra to an A → B model yields the species-associated spectra (SAS) along with singlet excited-state lifetimes of τ_{S1} = 1.02 ns for **3(Zn)** and τ_{S1} = 17.4 ns for **3** (Figure S29). Compound **2** and **2(Zn)** yielded TA spectra with similar features but with different lifetimes (Figure S30). The lifetimes for the four compounds and the relative enhancement of the decay rates due to EISC are summarized in Table 1. The ISC rate of zinc porphyrin in **3(Zn)** is increased by 66%, whereas a relatively moderate enhancement of 14% is observed for the ISC rate of free-base porphyrin in **3**. The higher increase in the ISC rate of **3(Zn)** indicates stronger exchange interaction between porphyrin triplet states and the radical, which agrees with the EPR measurement of observing quartet states for **3(Zn)**.

Table 1. Singlet Lifetimes ($\tau = 1/k$) for 2, 2(Zn), 3, and 3(Zn) and Increment of Rates for 3 and 3(Zn)

Compound	S1 Lifetimes (ns)	Increase of Decay Rate %
2(Zn)	1.69 ± 0.04	
3(Zn)	1.02 ± 0.02	65.7 ± 7.2
2	19.8 ± 0.1	
3	17.4 ± 0.1	13.8 ± 0.3

TA spectroscopy on **3(Cu)** and **3(Ni)** confirms the reasoning for the absence of a TREPR signal (Figures S31–32). The porphyrin excited state decays to the triplet in 0.46 and 1.01 ps for **3(Cu)** and **3(Ni)**, respectively, and the triplet decays on a much faster time scale with time constants of 1 and 5 ns, respectively, well within the instrument response of the EPR spectrometer. These enhanced rates relative to **3** and **3(Zn)** are most likely a result of EISC, leading to both faster porphyrin triplet formation and faster decay of the triplet excited state.[27,30,65]

CONCLUSIONS

We have synthesized a series of metalated porphyrins appended with the TEMPO SFR and investigated their photoexcited spin-state properties. The porphyrins were fully characterized and then investigated via a series of EPR experiments. TREPR spectra for the free-base porphyrin and Zn derivatives show distinguishable polarization patterns because of change in the magnitude of the exchange coupling between the porphyrin triplet state and the SFR. In addition,

https://dx.doi.org/10.1021/acs.jpca.0c03176
J. Phys. Chem. A 2020, 124, 6168−6176

EPR transient nutation experiments elucidated that metalation with Zn turns on the exchange coupling between the porphyrin triplet excited state and the TEMPO doublet state, yielding an overall quartet state. This change in exchange coupling through metalation was further confirmed by TA experiments, which determined a greater enhancement of ISC for the Zn porphyrin versus the free-base porphyrin when appended with TEMPO. Hence, we have realized a switchable exchange coupling through simple metalation. These results enable the possibility of employing metalation as a switchable coupler for multiqubit systems. Further studies will include varying the nature of the appended SFR, the number of appended SFRs, and the position of substitution (meso vs β) to expand our library of multispin porphyrins for potential quantum information applications.

■ ASSOCIATED CONTENT

Supporting Information

The Supporting Information is available free of charge at https://pubs.acs.org/doi/10.1021/acs.jpca.0c03176.

Experimental details, including synthesis, NMR, mass spectrometry, steady-state absorption and fluorescence, TA spectra and kinetics, CW-EPR and TREPR spectra, and echo-detected transient nutation data (PDF)

■ AUTHOR INFORMATION

Corresponding Author

Erin T. Chernick − *Institute für Organische Chemie, University of Tübingen, Tübingen 72076, Germany;* orcid.org/0000-0001-7352-6853; Email: erin.chernick@uni-tuebingen.de

Authors

Norbert Grzegorzek − *Institute für Organische Chemie, University of Tübingen, Tübingen 72076, Germany*

Haochuan Mao − *Department of Chemistry and Institute for Sustainability and Energy at Northwestern, Northwestern University, Evanston, Illinois 60208-3113, United States;* orcid.org/0000-0001-8742-089X

Patrick Michel − *Institute für Organische Chemie, University of Tübingen, Tübingen 72076, Germany*

Marc J. Junge − *Institute für Organische Chemie, University of Tübingen, Tübingen 72076, Germany*

Emmaline R. Lorenzo − *Department of Chemistry and Institute for Sustainability and Energy at Northwestern, Northwestern University, Evanston, Illinois 60208-3113, United States;* orcid.org/0000-0002-0445-3109

Ryan M. Young − *Department of Chemistry and Institute for Sustainability and Energy at Northwestern, Northwestern University, Evanston, Illinois 60208-3113, United States;* orcid.org/0000-0002-5108-0261

Matthew D. Krzyaniak − *Department of Chemistry and Institute for Sustainability and Energy at Northwestern, Northwestern University, Evanston, Illinois 60208-3113, United States;* orcid.org/0000-0002-8761-7323

Michael R. Wasielewski − *Department of Chemistry and Institute for Sustainability and Energy at Northwestern, Northwestern University, Evanston, Illinois 60208-3113, United States;* orcid.org/0000-0003-2920-5440

Complete contact information is available at: https://pubs.acs.org/10.1021/acs.jpca.0c03176

Author Contributions

N.G. and H.M. contributed equally. The manuscript was written through contributions of all authors. All authors have given approval to the final version of the manuscript.

Notes

The authors declare no competing financial interest.

■ ACKNOWLEDGMENTS

This work was supported by the National Science Foundation (NSF) for funding under grant number CHE-1900422 (M.R.W.). E.R.L. was supported by the National Science Foundation Graduate Research Fellowship (DGE-1842165).

■ REFERENCES

(1) Troiani, F.; Affronte, M. Molecular Spins for Quantum Information Technologies. *Chem. Soc. Rev.* **2011**, *40*, 3119−3129.

(2) Ivanov, K. L.; Wagenpfahl, A.; Deibel, C.; Matysik, J. Spin-Chemistry Concepts for Spintronics Scientists. *Beilstein J. Nanotechnol.* **2017**, *8*, 1427−1445.

(3) Sanvito, S. Molecular Spintronics. *Chem. Soc. Rev.* **2011**, *40*, 3336−3355.

(4) Hicks, R. G. What's New in Stable Radical Chemistry? *Org. Biomol. Chem.* **2007**, *5*, 1321−1338.

(5) Ratera, I.; Veciana, J. Playing with Organic Radicals as Building Blocks for Functional Molecular Materials. *Chem. Soc. Rev.* **2012**, *41*, 303−349.

(6) Kumar, S.; Kumar, Y.; Keshri, S.; Mukhopadhyay, P. Recent Advances in Organic Radicals and Their Magnetism. *Magnetochemistry* **2016**, *2*, 42.

(7) Mas-Torrent, M.; Crivillers, N.; Mugnaini, V.; Ratera, I.; Rovira, C.; Veciana, J. Organic Radicals on Surfaces: Towards Molecular Spintronics. *J. Mater. Chem.* **2009**, *19*, 1691−1695.

(8) Poggini, L.; Cucinotta, G.; Sorace, L.; Caneschi, A.; Gatteschi, D.; Sessoli, R.; Mannini, M. Nitronyl Nitroxide Radicals at the Interface: A Hybrid Architecture for Spintronics. *Rendiconti Lincei. Sci. Fis. Nat.* **2018**, *29*, 623−630.

(9) Lombardi, F.; Lodi, A.; Ma, J.; Liu, J.; Slota, M.; Narita, A.; Myers, W. K.; Müllen, K.; Feng, X.; Bogani, L. Quantum Units from the Topological Engineering of Molecular Graphenoids. *Science* **2019**, *366*, 1107.

(10) Rugg, B. K.; Krzyaniak, M. D.; Phelan, B. T.; Ratner, M. A.; Young, R. M.; Wasielewski, M. R. Photodriven Quantum Teleportation of an Electron Spin State in a Covalent Donor−Acceptor−Radical System. *Nat. Chem.* **2019**, *11*, 981−986.

(11) Olshansky, J. H.; Krzyaniak, M. D.; Young, R. M.; Wasielewski, M. R. Photogenerated Spin-Entangled Qubit (Radical) Pairs in DNA Hairpins: Observation of Spin Delocalization and Coherence. *J. Am. Chem. Soc.* **2019**, *141*, 2152−2160.

(12) Nelson, J. N.; Zhang, J.; Zhou, J.; Rugg, B. K.; Krzyaniak, M. D.; Wasielewski, M. R. CNOT Gate Operation on a Photogenerated Molecular Electron Spin-Qubit Pair. *J. Chem. Phys.* **2020**, *152*, 014503.

(13) Jurow, M.; Schuckman, A. E.; Batteas, J. D.; Drain, C. M. Porphyrins as Molecular Electronic Components of Functional Devices. *Coord. Chem. Rev.* **2010**, *254*, 2297−2310.

(14) Tran, T. T. H.; Chang, Y.-R.; Hoang, T. K. A.; Kuo, M.-Y.; Su, Y. O. Electrochemical Behavior of meso-Substituted Porphyrins: The Role of Cation Radicals to the Half-Wave Oxidation Potential Splitting. *J. Phys. Chem. A* **2016**, *120*, 5504−5511.

(15) Sano, S.; Sano, T.; Morishima, I.; Shiro, Y.; Maeda, Y. On the Mechanism of the Chemical and Enzymic Oxygenations of α-Oxyprotohemin IX to Fe. Biliverdin IX α. *Proc. Natl. Acad. Sci. U.S.A.* **1986**, *83*, 531.

(16) Shimizu, D.; Oh, J.; Furukawa, K.; Kim, D.; Osuka, A. Triarylporphyrin meso-Oxy Radicals: Remarkable Chemical Stabilities and Oxidation to Oxophlorin π-Cations. *J. Am. Chem. Soc.* **2015**, *137*, 15584−15594.

(17) Shimizu, D.; Osuka, A. Porphyrinoids as a Platform of Stable Radicals. *Chem. Sci.* **2018**, *9*, 1408−1423.
(18) Dommaschk, M.; Gutzeit, F.; Boretius, S.; Haag, R.; Herges, R. Coordination-Induced Spin-State-Switch (CISSS) in Water. *Chem. Commun.* **2014**, *50*, 12476−12478.
(19) Cotton, F. A., Wilkinson, G., Murillo, C. A., Bochmann, M. In *Advanced Inorganic Chemistry*, 6th ed.; Wiley Interscience: New York, 1999.
(20) Gnezdilov, O. I.; Mambetov, A. E.; Obynochny, A. A.; Salikhov, K. M. Time-Resolved EPR Study of Electron Spin Polarization and Spin Exchange in Mixed Solutions of Porphyrin Stable Free Radicals. *Appl. Magn. Reson.* **2003**, *25*, 157.
(21) Fujisawa, J.-I.; Ohba, Y.; Yamauchi, S. Electron-Spin Polarizations Generated from Interactions between Excited Triplet Porphyrins and Stable Radicals Studied by Time-Resolved Electron Paramagnetic Resonance. *J. Phys. Chem. A* **1997**, *101*, 434−439.
(22) Blank, A.; Levanon, H. Interaction between Polarized Triplets and Stable Radicals in Liquid Solutions. *J. Phys. Chem. A* **2001**, *105*, 4799.
(23) Blank, A.; Galili, T.; Levanon, H. Triplet Porphyrins as Donors in Intramolecular Electron Transfer and Their Intermolecular Interaction with Free Radicals. *J. Porphyrins Phthalocyanines* **2001**, *05*, 58−66.
(24) Poddutoori, P. K.; Pilkington, M.; Alberola, A.; Polo, V.; Warren, J. E.; van der Est, A. Spin−Spin Interactions in Porphyrin-Based Monoverdazyl Radical Hybrid Spin Systems. *Inorg. Chem.* **2010**, *49*, 3516−3524.
(25) Rakowsky, M. H.; More, K. M.; Kulikov, A. V.; Eaton, G. R.; Eaton, S. S. Time-Domain Electron Paramagnetic Resonance as a Probe of Electron-Electron Spin-Spin Interaction in Spin-Labeled Low-Spin Iron Porphyrins. *J. Am. Chem. Soc.* **1995**, *117*, 2049−2057.
(26) Teki, Y. Excited-State Dynamics of Non-Luminescent and Luminescent π-Radicals. *Chem.—Eur. J.* **2020**, *26*, 980−996.
(27) Buchachenko, A. L.; Berdinsky, V. L. Electron Spin Catalysis. *Chem. Rev.* **2002**, *102*, 603−612.
(28) Zarea, M.; Ratner, M. A.; Wasielewski, M. R. Spin Polarization Transfer by the Radical Pair Mechanism. *J. Chem. Phys.* **2015**, *143*, 054101.
(29) Kandrashkin, Y. E.; van der Est, A. Stimulated Electron Spin Polarization in Strongly Coupled Triplet−Doublet Spin Pairs. *Appl. Magn. Reson.* **2011**, *40*, 189−204.
(30) Colvin, M. T.; Giacobbe, E. M.; Cohen, B.; Miura, T.; Scott, A. M.; Wasielewski, M. R. Competitive Electron Transfer and Enhanced Intersystem Crossing in Photoexcited Covalent Tempo−Perylene-3,4:9,10-Bis(Dicarboximide) Dyads: Unusual Spin Polarization Resulting from the Radical−Triplet Interaction. *J. Phys. Chem. A* **2010**, *114*, 1741−1748.
(31) Gardner, D. M.; Chen, H.-F.; Krzyaniak, M. D.; Ratner, M. A.; Wasielewski, M. R. Large Dipolar Spin−Spin Interaction in a Photogenerated U-Shaped Triradical. *J. Phys. Chem. A* **2015**, *119*, 8040−8048.
(32) Colvin, M. T.; Smeigh, A. L.; Giacobbe, E. M.; Conron, S. M. M.; Ricks, A. B.; Wasielewski, M. R. Ultrafast Intersystem Crossing and Spin Dynamics of Zinc meso-Tetraphenylporphyrin Covalently Bound to Stable Radicals. *J. Phys. Chem. A* **2011**, *115*, 7538−7549.
(33) Dyar, S. M.; Margulies, E. A.; Horwitz, N. E.; Brown, K. E.; Krzyaniak, M. D.; Wasielewski, M. R. Photogenerated Quartet State Formation in a Compact Ring-Fused Perylene-Nitroxide. *J. Phys. Chem. B* **2015**, *119*, 13560−13569.
(34) Giacobbe, E. M.; Mi, Q.; Colvin, M. T.; Cohen, B.; Ramanan, C.; Scott, A. M.; Yeganeh, S.; Marks, T. J.; Ratner, M. A.; Wasielewski, M. R. Ultrafast Intersystem Crossing and Spin Dynamics of Photoexcited Perylene-3,4:9,10-Bis(Dicarboximide) Covalently Linked to a Nitroxide Radical at Fixed Distances. *J. Am. Chem. Soc.* **2009**, *131*, 3700−3712.
(35) Gütlich, P., Goodwin, H. A. Spin Crossover—an Overall Perspective. In *Spin Crossover in Transition Metal Compounds I*; Gütlich, P., Goodwin, H. A., Eds.; Springer: Berlin, Heidelberg, 2004; pp 1−47.
(36) Balch, A. L.; Noll, B. C.; Phillips, S. L.; Reid, S. M.; Zovinka, E. P. Nickel(II) Complexes of the Octaethyloxophlorin Dianion and Octaethyloxophlorin Radical Dianion. *Inorg. Chem.* **1993**, *32*, 4730−4736.
(37) Stähler, C.; Shimizu, D.; Yoshida, K.; Furukawa, K.; Herges, R.; Osuka, A. Stable Ni^{II} Porphyrin meso-Oxy Radical with a Quartet Ground State. *Chem.—Eur. J.* **2017**, *23*, 7217−7220.
(38) Chernick, E. T.; Casillas, R.; Zirzlmeier, J.; Gardner, D. M.; Gruber, M.; Kropp, H.; Meyer, K.; Wasielewski, M. R.; Guldi, D. M.; Tykwinski, R. R. Pentacene Appended to a Tempo Stable Free Radical: The Effect of Magnetic Exchange Coupling on Photoexcited Pentacene. *J. Am. Chem. Soc.* **2015**, *137*, 857−863.
(39) Weiss, E. A.; Chernick, E. T.; Wasielewski, M. R. Modulation of Radical Ion Pair Lifetimes by the Presence of a Third Spin in Rodlike Donor−Acceptor Triads. *J. Am. Chem. Soc.* **2004**, *126*, 2326−2327.
(40) Mi, Q.; Chernick, E. T.; McCamant, D. W.; Weiss, E. A.; Ratner, M. A.; Wasielewski, M. R. Spin Dynamics of Photogenerated Triradicals in Fixed Distance Electron Donor−Chromophore−Acceptor−TEMPO Molecules. *J. Phys. Chem. A* **2006**, *110*, 7323−7333.
(41) Chernick, E. T.; Mi, Q.; Vega, A. M.; Lockard, J. V.; Ratner, M. A.; Wasielewski, M. R. Controlling Electron Transfer Dynamics in Donor−Bridge−Acceptor Molecules by Increasing Unpaired Spin Density on the Bridge. *J. Phys. Chem. B* **2007**, *111*, 6728−6737.
(42) Chernick, E. T.; Mi, Q.; Kelley, R. F.; Weiss, E. A.; Jones, B. A.; Marks, T. J.; Ratner, M. A.; Wasielewski, M. R. Electron Donor−Bridge−Acceptor Molecules with Bridging Nitronyl Nitroxide Radicals: Influence of a Third Spin on Charge- and Spin-Transfer Dynamics. *J. Am. Chem. Soc.* **2006**, *128*, 4356−4364.
(43) McLees, B. D.; Caughey, W. S. Substituted Deuteroporphyrins. V. Structures, Stabilities, and Properties of Nickel(Ii) Complexes with Axial Ligands. *Biochemistry* **1968**, *7*, 642−652.
(44) Thies, S.; Bornholdt, C.; Köhler, F.; Sönnichsen, F. D.; Näther, C.; Tuczek, F.; Herges, R. Coordination-Induced Spin Crossover (Cisco) through Axial Bonding of Substituted Pyridines to Nickel−Porphyrins: Σ-Donor Versus Π-Acceptor Effects. *Chem.—Eur. J.* **2010**, *16*, 10074−10083.
(45) Walker, F. A.; Hui, E.; Walker, J. M. Electronic Effects in Transition Metal Porphyrins. I. Reaction of Piperidine with a Series of Para- and Meta-Substituted Nickel(II) and Vanadium(IV) Tetraphenylporphyrins. *J. Am. Chem. Soc.* **1975**, *97*, 2390−2397.
(46) Rothemund, P. Formation of Porphyrins from Pyrrole and Aldehydes. *J. Am. Chem. Soc.* **1935**, *57*, 2010−2011.
(47) Adler, A. D.; Longo, F. R.; Shergalis, W. Mechanistic Investigations of Porphyrin Syntheses. I. Preliminary Studies on ms-Tetraphenylporphin. *J. Am. Chem. Soc.* **1964**, *86*, 3145−3149.
(48) Lindsey, J. S.; Hsu, H. C.; Schreiman, I. C. Synthesis of Tetraphenylporphyrins under Very Mild Conditions. *Tetrahedron Lett.* **1986**, *27*, 4969−4970.
(49) Heo, P. Y.; Lee, C. H. Facile Syntheses of Modified Tripyrranes and Their Application to the Syntheses of Regioisomerically Pure Porphyrin Derivatives. *Bull. Korean Chem. Soc.* **1996**, *17*, 515−520.
(50) Lee, C.-H.; Li, F.; Iwamoto, K.; Dadok, J.; Bothner-By, A. A.; Lindsey, J. S. Synthetic Approaches to Regioisomerically Pure Porphyrins Bearing 4 Different meso-substituents. *Tetrahedron* **1995**, *51*, 11645−11672.
(51) Lee, C.-H.; S. Lindsey, J. One-Flask Synthesis of Meso-substituted Dipyrromethanes and Their Application in the Synthesis of Trans-Substituted Porphyrin Building-Blocks. *Tetrahedron* **1994**, *50*, 11427−11440.
(52) Lindsey, J. S. Synthetic Routes to meso-Patterned Porphyrins. *Acc. Chem. Res.* **2010**, *43*, 300−311.
(53) Rao, P. D.; Littler, B. J.; Geier, G. R.; Lindsey, J. S. Efficient Synthesis of Monoacyl Dipyrromethanes and Their Use in the Preparation of Sterically Unhindered trans-Porphyrins. *J. Org. Chem.* **2000**, *65*, 1084−1092.
(54) Senge, M. O. Nucleophilic Substitution as a Tool for the Synthesis of Unsymmetrical Porphyrins. *Acc. Chem. Res.* **2005**, *38*, 733−743.

https://dx.doi.org/10.1021/acs.jpca.0c03176
J. Phys. Chem. A 2020, 124, 6168−6176

(55) Wallace, D. M.; Leung, S. H.; Senge, M. O.; Smith, K. M. Rational Tetraarylporphyrin Syntheses - Tetraarylporphyrins from the Macdonald Route. *J. Org. Chem.* **1993**, *58*, 7245−7257.
(56) Kooriyaden, F. R.; Sujatha, S.; Varghese, B.; Arunkumar, C. Synthesis of Electron-Deficient Fluorinated Porphyrins through Scrambling: Characterization and Quantitative Crystal Structure Analysis. *J. Fluorine Chem.* **2015**, *170*, 10−16.
(57) Jeremy, K. M., Sanders, N. B., Clyde-Watson, S. L. D. Z., Hawley, J.C., Kim, H.-J., Mak, C.C., Webb, S. J. *The Porphyrin Handbook*; Academic Press, Elsever Science, 1999; Vol. 3.
(58) The reaction to form the imine bond between the porphyrin and TEMPO radical is quantitative in nature. However, after recrystallization, the porphyrin aldehyde precursors 2, 2(Ni), 2(Zn) and 2(Cu) still contain residual solvent so we cannot report quantitative yields for the porphryin radicals 3, 3(Ni), 3(Zn) and 3(Cu).
(59) Gouterman, M. Spectra of Porphyrins. *J. Mol. Spectrosc.* **1961**, *6*, 138−163.
(60) Krzystek, J.; Park, J.-H.; Meisel, M. W.; Hitchman, M. A.; Stratemeier, H.; Brunel, L.-C.; Telser, J. EPR Spectra from "EPR-Silent" Species: High-Frequency and High-Field EPR Spectroscopy of Pseudotetrahedral Complexes of Nickel(II). *Inorg. Chem.* **2002**, *41*, 4478−4487.
(61) Greiner, S. P.; Rowlands, D. L.; Kreilick, R. W.; EPR; ENDOR Study. of Selected Porphyrin- and Phthalocyanine-Copper Complexes. *J. Phys. Chem.* **1992**, *96*, 9132−9139.
(62) Yu, C.-J.; Krzyaniak, M. D.; Fataftah, M. S.; Wasielewski, M. R.; Freedman, D. E. A Concentrated Array of Copper Porphyrin Candidate Qubits. *Chem. Sci.* **2019**, *10*, 1702−1708.
(63) Gouterman, M. Study of the Effects of Substitution on the Absorption Spectra of Porphin. *J. Chem. Phys.* **1959**, *30*, 1139−1161.
(64) Khudyakov, I. V.; Serebrennikov, Y. A.; Turro, N. J. Spin-Orbit Coupling in Free-Radical Reactions: On the Way to Heavy Elements. *Chem. Rev.* **1993**, *93*, 537−570.
(65) Yeganeh, S.; Wasielewski, M. R.; Ratner, M. A. Enhanced Intersystem Crossing in Three-Spin Systems: A Perturbation Theory Treatment. *J. Am. Chem. Soc.* **2009**, *131*, 2268−2273.
(66) Thurnauer, M. C.; Katz, J. J.; Norris, J. R. The Triplet State in Bacterial Photosynthesis: Possible Mechanisms of the Primary Photo-Act. *Proc. Natl. Acad. Sci. U.S.A.* **1975**, *72*, 3270.
(67) Scherz, A.; Orbach, N.; Levanon, H. Kinetic Study of the Photoexcited Triplet State of Free Base Porphyrins by EPR. *Isr. J. Chem.* **1974**, *12*, 1037−1048.
(68) Barbon, A.; Farra, M. G. D.; Albertini, M.; Bolzonello, L.; Orian, L.; Di Valentin, M.; Di Valentin, M. Comprehensive Investigation of the Triplet State Electronic Structure of Free-Base 5,10,15,&nospace;20-Tetrakis(4-Sulfonatophenyl)Porphyrin by a Combined Advanced EPR and Theoretical Approach. *J. Chem. Phys.* **2020**, *152*, 034201.
(69) van der Est, A.; Asano-Someda, M.; Ragogna, P.; Kaizu, Y. Light-Induced Electron Spin Polarization of a Weakly Coupled Triplet−Doublet Spin Pair in a Covalently Linked Porphyrin Dimer. *J. Phys. Chem. A* **2002**, *106*, 8531−8542.
(70) Kandrashkin, Y. E.; van der Est, A. The Triplet Mechanism of Electron Spin Polarization in Moderately Coupled Triplet-Doublet Rigid Complexes as a Source of the Enhanced +1/2 <–> -1/2 Transitions. *J. Chem. Phys.* **2019**, *151*, 184301.
(71) Kooter, J. A.; Van der Waals, J. H. The Metastable Triplet State of Zinc Porphin and Magnesium Porphin: A Study by E.S.R. In an N-Octane Crystal at 1·4 K. *Mol. Phys.* **1979**, *37*, 997−1013.
(72) Gonen, O.; Levanon, H. Time-Resolved EPR Spectroscopy of Electron Spin Polarized ZnTPP Triplets Oriented in a Liquid Crystal. *J. Phys. Chem.* **1985**, *89*, 1637−1643.
(73) Richert, S.; Tait, C. E.; Timmel, C. R. Delocalisation of Photoexcited Triplet States Probed by Transient EPR and Hyperfine Spectroscopy. *J. Magn. Reson.* **2017**, *280*, 103−116.
(74) Richert, S.; Limburg, B.; Anderson, H. L.; Timmel, C. R. On the Influence of the Bridge on Triplet State Delocalization in Linear Porphyrin Oligomers. *J. Am. Chem. Soc.* **2017**, *139*, 12003−12008.
(75) Tait, C. E.; Neuhaus, P.; Peeks, M. D.; Anderson, H. L.; Timmel, C. R. Transient EPR Reveals Triplet State Delocalization in a Series of Cyclic and Linear Π-Conjugated Porphyrin Oligomers. *J. Am. Chem. Soc.* **2015**, *137*, 8284−8293.
(76) Isoya, J.; Kanda, H.; Norris, J. R.; Tang, J.; Bowman, M. K. Fourier-Transform and Continuous-Wave EPR Studies of Nickel in Synthetic Diamond: Site and Spin Multiplicity. *Phys. Rev. B Condens. Matter* **1990**, *41*, 3905−3913.
(77) Astashkin, A. V.; Schweiger, A. Electron-Spin Transient Nutation: A New Approach to Simplify the Interpretation of ESR Spectra. *Chem. Phys. Lett.* **1990**, *174*, 595−602.
(78) Sukhanov, A. A.; Konov, K. B.; Salikhov, K. M.; Voronkova, V. K.; Mikhalitsyna, E. A.; Tyurin, V. S. Time-Resolved Continuous-Wave and Pulse EPR. Investigation of Photoinduced States of Zinc Porphyrin Linked with an Ethylenediamine Copper Complex. *Appl. Magn. Reson.* **2015**, *46*, 1199−1220.
(79) Matsuzawa, N.; Ata, M.; Dixon, D. A. Density Functional Theory Prediction of the Second-Order Hyperpolarizability of Metalloporphines. *J. Phys. Chem.* **1995**, *99*, 7698−7706.
(80) Wertz, J. E., Bolton, J. R. *Electron Spin Resonance: Elementary Theory and Practical Applications*; McGraw-Hill: New York, 1972.
(81) Clarke, R. H.; Connors, R. E.; Schaafsma, T. J.; Kleibeuker, J. F.; Platenkamp, R. J. The Triplet State of Chlorophylls. *J. Am. Chem. Soc.* **1976**, *98*, 3674−3677.
(82) Langhoff, S. R.; Davidson, E. R.; Gouterman, M.; Leenstra, W. R.; Kwiram, A. L. Zero Field Splitting of the Triplet State of Porphyrins. II. *J. Chem. Phys.* **1975**, *62*, 169−176.
(83) Fleischer, E. B.; Miller, C. K.; Webb, L. E. Crystal Molecular Structures of Some Metal Tetraphenylporphines. *J. Am. Chem. Soc.* **1964**, *86*, 2342−2347.
(84) Kay, C. W. M. The Electronic Structure of the Photoexcited Triplet State of Free-Base (Tetraphenyl)Porphyrin by Time-Resolved Electron−Nuclear Double Resonance and Density Functional Theory. *J. Am. Chem. Soc.* **2003**, *125*, 13861−13867.
(85) Liu, Y.; Villamena, F. A.; Rockenbauer, A.; Song, Y.; Zweier, J. L. Structural Factors Controlling the Spin−Spin Exchange Coupling: Epr Spectroscopic Studies of Highly Asymmetric Trityl−Nitroxide Biradicals. *J. Am. Chem. Soc.* **2013**, *135*, 2350−2356.
(86) Liu, Y.; Villamena, F. A.; Rockenbauer, A.; Zweier, J. L. Trityl-Nitroxide Biradicals as Unique Molecular Probes for the Simultaneous Measurement of Redox Status and Oxygenation. *Chem. Commun.* **2010**, *46*, 628−630.

https://dx.doi.org/10.1021/acs.jpca.0c03176
J. Phys. Chem. A 2020, 124, 6168−6176